

Indices for capturing spatial patterns and their evolution in time, with application to European hake (*Merluccius merluccius*) in the Bay of Biscay

Mathieu Woillez, Jean-Charles Poulard, Jacques Rivoirard, Pierre Petitgas, and Nicolas Bez

Woillez, M., Poulard, J.-C., Rivoirard, J., Petitgas, P., and Bez, N. 2007. Indices for capturing spatial patterns and their evolution in time, with application to European hake (*Merluccius merluccius*) in the Bay of Biscay. – ICES Journal of Marine Science, 64: 537–550.

A series of candidate statistical indices is used in an attempt to capture spatial patterns of fish populations from research survey data. To handle diffuse population limits, indices are designed not to depend on arbitrary delineation of the domain. They characterize the location (centre of gravity and spatial patches), the occupation of space (inertia, isotropy, positive area, spreading area, and equivalent area), statistical dispersion (Gini index and coefficient of variation of strictly positive densities), and microstructure. Collocation between different ages and years is summarized by a global index of collocation. Indices are estimated for hake from a bottom-trawl data series in the Bay of Biscay in autumn of 1987–2004. The study provides a detailed description of the spatial patterns of different hake age groups, age 3 appearing to be a turning point in these dynamics. Capturing spatial patterns through indices allows the comparison of surveyed populations and identification of trends and outliers in the time-series. Spatial indices are used in a multivariate approach to obtain an overview of the relationships between the different spatial indices characterizing the spatial behaviour of six age groups of hake, and to assess their persistence through time.

Keywords: Bay of Biscay, European hake, spatial indices.

Received 23 August 2006; accepted 1 February 2007.

M. Woillez and J. Rivoirard: Centre de Géosciences/Géostatistique, Ecole des Mines de Paris, 35 rue Saint-Honoré, 77305 Fontainebleau Cedex, France. J.-C. Poulard and P. Petitgas: IFREMER, Department Ecology and Model for Fisheries, rue de l'île d'Yeu, BP 21105, 44311 Nantes Cedex 03, France. N. Bez: IRD, Centre de Recherche Halieutique Méditerranéenne et Tropicale, rue Jean Monnet, BP171, 34203 Sète Cedex, France. Correspondence to M. Woillez: tel: +33 164 694776; fax: +33 164 694705; e-mail: mathieu.woillez@ensmp.fr

Introduction

Spatial patterns of fish populations have been the subject of many ecological investigations, and changes in the spatial distribution of depleted stocks have been demonstrated. MacCall (1990) suggests the existence of a relationship between geographic distribution and population abundance that may result from density-dependent habitat selection. It is also widely believed that global climate warming (McFarlane *et al.*, 2000; Roessig *et al.*, 2004) and fishing (Greenstreet and Hall, 1996; Garrison and Link, 2000) influence the spatial patterns of fish populations.

Our aim was to seek a series of basic statistics or indices that could help to capture the spatial patterns of fish populations. Spatial indices may be useful in detecting changes over time, using survey data obtained from monitoring cruises, and such indices have occasionally been used for fish populations. For instance, spatial location is often summarized by the centre of gravity (CG) and the inertia (Bez, 1997), also referred to as the distributional centroid and the variance of spatial distribution (Hollowed, 1992). These two parameters have been used to demonstrate shifts in spatial distributions from survey data (Atkinson *et al.*, 1997). An ellipse shows the centre, the main structuring directions of the geographical distribution, and the extent of dispersion around the centre (Murawski and Finn, 1988; Kendall and Picquelle, 1989; Brodie *et al.*, 1998).

The CG represents the mean location of a population, i.e. the mean of the locations of its individuals, and the inertia is the corresponding variance. It is possible to describe the statistical distribution of the values of any spatial parameter corresponding to the individuals of a population, e.g. the mean depth, the variance in the depths of individuals, the mean temperature, and the variance in temperatures (Bez, 1997). When such individual-based statistics are computed, the parameter values at data locations are weighted by the population densities at corresponding locations. It is important to realize that a sample location with zero population density has a numerical contribution equal to zero in such individual-based statistics (but to say that it has no influence would be untrue; the statistics would be different if the density at that point were not zero) (Bez and Rivoirard, 2001). Similarly, spatially distributed abundance depends on all values of population density, being the sum of them, but the contribution of zero densities to abundance is zero.

Other spatial indices characterizing the distribution or the extension of a population from survey data have been used. Some are based on an estimation of the area over which density values exceed a specific level, a threshold that can be an absolute value, e.g. a long-term percentile abundance (Crecco and Overholtz, 1990; Swain and Wade, 1993), or a percentage of the population (Swain and Sinclair, 1994; Swain and Morin, 1996).

Others are cumulative frequencies. Marshall and Frank (1994) used cumulative frequency plots to determine the centre of a distribution. Myers and Cadigan (1995) used a Lorenz curve to relate percentage biomass to percentage area, and they show increases in concentration of cod (*Gadus morhua*) over time using the Gini index (Gini, 1921). An equivalent version of the Lorenz curve is given by the geostatistical aggregation curve of mining geostatistics, which is a particularly useful tool for handling the effect on the curves of the support (a point, a surface, or a volume) on which the variable is measured or defined (Matheron, 1981). This has been proposed in fisheries to look at the mode of aggregation of fish when abundance changes (Petitgas, 1998).

The curves listed above are basically different ways to represent the histogram of values of population density. In particular, although they are computed from spatially distributed values of population density, they would be unchanged by permutation of the data locations. This is also the case for mean population density over a domain, and for the basic statistics that can be used to describe the statistical dispersion of population densities within the domain: the variance, the standard deviation, the coefficient of variation (CV), and the Gini index. A drawback of such basic statistics is that they depend on delineation of the domain, particularly when the population has diffuse limits and one has to select which zero sample values to include within the domain. In a case where the same domain is used to follow evolution in time, these statistics are affected by the zero densities that may be present in a time-varying proportion within the domain.

Here, we favour the use of indices that are not dependent on an arbitrary delineation of the domain and in which the values of zero density have a null contribution, as is the case for individual-based statistics. A series of spatial indices is therefore selected, intended to help capture the spatial patterns of a population in a simple manner. This is illustrated first in a mono- and bivariate approach, then in a multivariate approach using European hake (*Merluccius merluccius*) data collected during annual groundfish surveys carried out by Institut Français de Recherche pour l'Exploitation de la Mer (IFREMER) in the Bay of Biscay. Finally, the set of indices is used to describe interannual variability in different age groups of the hake population, as observed during the surveys.

Material and methods

Data

Hake are commercially important in the Bay of Biscay. In addition to a directed fishery for the species for human consumption, juvenile hake are taken as bycatch by trawlers targeting *Nephrops* (Drouineau *et al.*, 2006).

Data were collected during 15 groundfish surveys carried out by IFREMER from October to December of the years 1987–2004 (EVHOE series, with gaps in 1991, 1993, and 1996), on the eastern continental shelf of the Bay of Biscay (ICES, 1997; Poulard *et al.*, 2003; Poulard and Blanchard, 2005). The study area was between 48°30'N and 43°30'N, and the depth ranged from 15 to 600 m. Sampling was stratified according to latitude and depth, and the number of hauls per survey varied between 70 and 139.

A 36/47 Grande Ouverture Verticale (GOV) trawl was used with a codend liner of 20-mm mesh. Haul duration was 30 min at a towing speed of four knots, mainly in daylight. Catch weights and numbers were recorded for all species. Hake sex and total length were recorded, and otoliths were extracted and

examined in the laboratory to build age–length keys (ALKs) by sex. These keys were used to transform the length frequencies observed at each trawl station into age frequencies.

For our purpose, hake densities were disaggregated by age (0–5+) and expressed in numbers of fish caught per hour trawled. To calculate the index of abundance, we assumed that the area swept in 30 min of trawling was 0.02 square nautical miles.

Spatial indices

CG and inertia

The CG is the mean location of the population and also the mean location of an individual fish taken at random in the field. Inertia, the mean square distance between such an individual fish and the CG, describes the dispersion of the population around its CG.

Let x be a point in two-dimensional space [short for the usual two-dimension notation (x, y)], and $z(x)$ be the density of population at location x . Then, the total abundance of the population (Q) is calculated from

$$Q = \int z(x) dx, \quad (1)$$

and the probability density function of the location \underline{x} of a random individual is $z(x)/Q$. The CG is

$$CG = E(\underline{x}) = \int x \frac{z(x)}{Q} dx = \frac{\int xz(x) dx}{\int z(x) dx}, \quad (2)$$

and the inertia (I) is

$$I = \text{Var}(\underline{x}) = \frac{\int (x - CG)^2 z(x) dx}{\int z(x) dx}. \quad (3)$$

In practice, these statistics are estimated from the data through discrete summations over sample locations. In the case of irregular sampling, areas of influence around samples are used as weighting factors. Practically, from sample values z_i at locations x_i , with areas of influence s_i , we have

$$CG = \frac{\sum_{i=1}^N x_i s_i z_i}{\sum_{i=1}^N s_i z_i}, \quad \text{and} \quad (4)$$

$$I = \frac{\sum_{i=1}^N (x_i - CG)^2 s_i z_i}{\sum_{i=1}^N s_i z_i}. \quad (5)$$

The area of influence of a sample location is defined as the area made up of the points in space that are closer to this sample than to others. It can be evaluated by overlying a very fine regular grid and counting grid points closer to the sample. Known or supposed boundaries (e.g. land, a limit distance of influence from a sample location) of the sampled population may be used.

Global index of collocation

The global index of collocation looks at how geographically distinct two populations are by comparing the distance between their CGs and the mean distance between individual fish taken

at random and independently from each population (Bez and Rivoirard, 2000). Let us consider two populations with densities $z_1(x)$ and $z_2(x)$ at point x , with ΔCG separating their CGs, and I_1 and I_2 their respective inertias. Then, the global index of collocation (GIC) is

$$\text{GIC} = 1 - \frac{\Delta CG^2}{\Delta CG^2 + I_1 + I_2}, \quad (6)$$

or 1 if $\Delta CG^2 = I_1 = I_2 = 0$. The spatial index ranges between 0, in the extreme case where each population is concentrated on a single but different location (inertia = 0), and 1, where the two CGs coincide and the inertias have any non-negative values.

Anisotropy and isotropy

In general, the dispersion of a population around its CG is not necessarily identical in every direction of space (i.e. isotropic). Therefore, in two dimensions, the total inertia of a population can be decomposed on its two principal axes, orthogonal to each other, explaining, respectively, the maximum and the minimum parts of overall inertia. This can be obtained from a principal component analysis of the coordinates of the fish constituting the population (i.e. the coordinates of the samples weighted by the densities observed). The square root of the inertia along a given axis (i.e. of the eigenvalue) gives the standard deviation of the projection of the location of the population along that axis. This can be represented conveniently on a map as a cross depicting the two principal directions. Anisotropy exists when there is a difference in inertia between the two directions. This can be summarized by the anisotropy index being equal to the square root ratio between the maximum and the minimum of the inertia. The more it exceeds 1, the greater will be the contrast between the directions as a result of anisotropy. Similarly, an index of isotropy can be defined as the inverse of anisotropy, ranging more conveniently from 0 to 1:

$$\text{Isotropy} = \sqrt{\frac{I_{\min}}{I_{\max}}}. \quad (7)$$

Number of spatial patches

The spatial distribution of a fish population in a given area may include spatial patches that are bigger than a fish school. An algorithm has been written to identify spatial patches, based on the choice of a threshold distance: a sample is attributed to a patch according to the value observed and to the distance of its location from patches previously identified. The algorithm starts from the value displaying the maximum density $z(x)$, and considers every other sample in decreasing order of density. The maximum value initiates the first patch. Then, the current sample value is attributed to the nearest patch, if the distance to its CG is smaller than the threshold distance. Otherwise, the current sample value defines a new patch. Spatial patches whose abundance is $>10\%$ of overall abundance are retained. The summary index is the number of patches.

Positive area

The positive area (PA) is the area occupied by fish densities >0 . It is expressed in square nautical miles and estimated from data as the sum of the areas of influence around samples where there

are fish densities >0 :

$$\text{PA} = \sum_i s_i I_{z_i > 0}. \quad (8)$$

Zero values of density make no contribution to the positive area. However, the positive area is highly sensitive to low values of density, because very small or high-density values make similar contributions to the positive area.

Spreading area and Gini index

The spreading area (SA) is an index related to the Gini index, but which has the advantage over the Gini index of having no contribution from zero values of density. The Gini index (ranging from 0 to 1) equals twice the area between the Lorenz curve (the graphical representation of the cumulative proportion of abundance vs. the cumulative area proportion) and the 1:1 line to which it would be reduced if all densities were the same. It depends on the proportion of zero-density values within the domain considered. In contrast, we define the SA as follows. Let T be the cumulated area occupied by the density values, ranked in decreasing order, $Q(T)$ the corresponding cumulated abundance, and Q the overall abundance. The SA (expressed in square nautical miles) is then simply defined as twice the area below the curve expressing $(Q - Q(T))/Q$ as a function of T :

$$\text{SA} = 2 \int \frac{Q - Q(T)}{Q} dT. \quad (9)$$

The zero-density area has no contribution to the SA. As $(Q - Q(T))/Q$ decreases from 1 to 0 and is convex, the SA is less than the PA. It equals the PA when the population is evenly spread at constant density. When normalizing the SA by the PA, we have the simple relation:

$$\frac{\text{SA}}{\text{PA}} + G_0 = 1, \quad (10)$$

where G_0 is the Gini index computed from density values >0 .

Equivalent area and CV

A transitive geostatistical approach (Matheron, 1971) can be used to describe the spatial distribution of a fish population when it includes a few large values of density, and when it is difficult to delimit a domain with homogeneous variations (Bez *et al.*, 1995, 1997). The spatial structure is then represented by a (transitive) covariogram, a function of the distance between two locations:

$$g(h) = \int z(x)z(x+h)dh. \quad (11)$$

Here, the equivalent area (EA) is defined as the integral range of the covariogram:

$$\text{EA} = \frac{\int g(h)dh}{g(0)} = \frac{Q^2}{g(0)} = \frac{Q^2}{\int z(x)^2 dx} = \frac{(\int z(x)dx)^2}{\int z(x)^2 dx}. \quad (12)$$

It can also be written:

$$EA = \frac{Q}{\int z(x)(z(x)/Q)dx} \tag{13}$$

It represents the area that would be covered by the population if all individuals had the same density, equal to the mean density per individual [the denominator in Equation (13)].

Practically, in the discrete case with sample values z_i and areas of influence s_i , Equation (12) yields:

$$EA = \frac{(\sum_{i=1}^N s_i z_i)^2}{\sum_{i=1}^N s_i z_i^2} \tag{14}$$

The EA ranges from 0 to the PA. It would be equal to the PA if all strictly positive values of density were the same. Their ratio is related to the CV of the strictly positive values of density through the relation:

$$\frac{PA}{EA} = 1 + CV_0^2, \tag{15}$$

where CV_0 is the CV of density values >0 . Thus,

$$EA = \frac{Q^2}{\int z(x)^2 dx} = \frac{PA^2 m_0^2}{PA(m_0^2 + \sigma_0^2)} = \frac{PA}{(1 + CV_0^2)} \tag{16}$$

Inequalities exist between the spreading area and the equivalent area; these are detailed in the Appendix.

Microstructure index

The microstructure index (MI) is taken as the relative decrease of the covariogram between distance zero and a distance h_0 chosen to represent the mean lag between samples:

$$MI = \frac{(g(0) - g(h_0))}{g(0)} \tag{17}$$

It measures the relative importance of structural components at a scale smaller than the sample lag (including random noise), and lies between 0 and 1. Values close to 0 correspond to a very regular, well-structured density surface, and values close to 1 correspond to a highly irregular, poorly structured, density surface.

Distribution and mean of a population parameter

This refers to the distribution and the mean of a spatially distributed parameter, weighted by fish density. In the hake example, these are used to summarize the depth and type of sediments experienced by the fish.

Analyses

Bubble plots of fish density samples, time-series of spatial indices, box plots of spatial indices, plots of CG, and tables of global indices of collocation were used to explore the data. Subsequently, pairwise scatterplots of the spatial indices were examined.

To summarize the spatial distribution of the population and to identify differences between years, an overall multivariate analysis was performed on the 15 survey years, on the six age groups from 0

(hake born during the first months of the year) to 5+ y old (age groups 0–5 +), and on a total of 11 spatial indices: the longitude of the CG, the latitude of the CG, inertia, isotropy, the number of patches, PA, SA, the Gini index of positive densities, EA, the CV of positive densities, and the MI. Multiple factor analysis (MFA) (Escofier and Pagès, 1994; Pagès and Husson, 2001; Stanimivora et al., 2005) offers a theoretical framework suited to investigation of the reproducibility of multivariate structures.

MFA was performed using SPAD software (DECISIA, 2003) to provide a simultaneous representation of the six age groups during 15 surveys. MFA first performs a separate principal component analysis (PCA) for each group of variables (defined by years). Each group is then weighted by the inverse of the first eigenvalue of its separate analysis. This balances inertia between the different groups and therefore their influences in the PCA of the entire weighted matrix, performed to study the different groups of variables in a unique reference space. The correlation between the overall cloud (defined by all variables) and partial clouds (defined by the variables of each group) indicates whether there is a common structure between different groups of variables.

There are different stages of our analysis. The first, interstructure analysis, studies the relationships between groups (here, years) of variables (here, spatial indices) from an holistic point of view. The second, referred to as a compromise analysis, studies the proximities between individuals (here, age groups), based on the weighted means of the proximities associated with each group of variables. The third stage, intrastructure analysis, consists of an analytical study of the relationships among the variables and the proximities among the individual fish in the different groups of variables.

Generally, our starting thesis is that the spatial distribution of a population is a combination of the spatial distributions of each of its main components (age groups or juveniles/adults, for instance) allowing for some differences between them. The biological requirements of each component, which should be constant from year to year, result in specific spatial features for each component’s distribution. A persisting relationship between components is expected, with some interannual variability.

Results

Spatial patterns

Spatial indices are applied to describe spatial patterns in the hake population (Table 1) inhabiting the eastern continental shelf of the Bay of Biscay in autumn of the years 1987–2004. To obtain a series of indices reliable over years, we needed to compute them inside the same polygonal domain (Figure 1) that delineated the maximal sampled area. The computations for a given year are

Table 1. Basic statistics of abundance and length-at-age of hake in the Bay of Biscay, 1987–2004.

Age	Abundance (thousand fish)		Length (cm)			
	Mean	s.d.	Mean	s.d.	Minimum	Maximum
0	139 189	95 039	14.7	2.4	5	23
1	17 154	8 117	21.1	2.5	15	29
2	7 915	3 462	31.1	2.8	23	39
3	5 326	3 035	38.4	2.4	31	44
4	1 561	1 023	44.9	2.1	40	51
5+	1 025	894	55.8	7.7	44	108

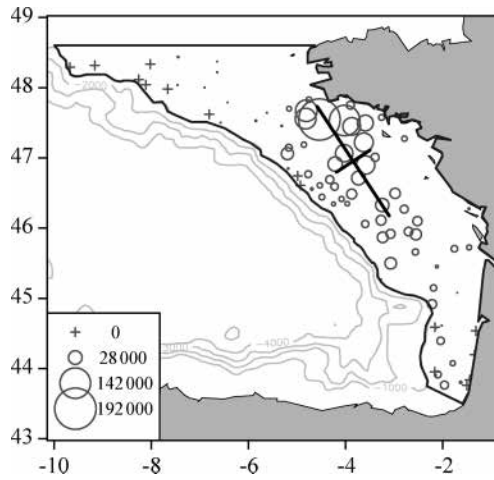


Figure 1. Bubble plot, CG, and axes of inertia of hake aged 0 densities found during the French groundfish survey by the RV “Thalassa” in 2004. The bold line delineates the polygonal domain corresponding to the maximal sampled area through the 15 surveys considered in the study.

weighted by the area of influence attributed to each sample for that year, the spatial population being closed by zero-density values, if any, or by the limits of the domain. There were a few gaps in sampling, e.g. through bad weather, which might cause a bias in the indices. The influence of each sample was limited to 25 nautical miles in order not to extrapolate its value unduly.

The location of the population is summarized by the position of the CG for the different age groups over the study period (Figure 2). The CGs of hake aged 0 were close to each other and extended linearly throughout the muddy substrata. The latitudinal range was ~140 km, but this reduced to ~100 km if the outlier year 2000 was excluded. Similarly, the longitudinal range decreased from ~75 to ~50 km if the year 2000 was excluded. We could find nothing in the information on the 2000 survey (start or end dates, spatial distribution of sampling effort, etc.) that could explain its outlier status. The CGs of hake aged 1 y revealed that they were distributed between the coast and the area occupied by 0-y-old hake and that 2-y-olds were slightly farther west. The CGs of hake aged 3 y were more variable in

terms of longitude (a range of 140 km), but were around the southern portion of the distribution of CGs of age groups 0–2. Scattering along the shelf edge and shifts to the west were more pronounced for age groups 4 and 5+ (Figures 2 and 3b). Additionally, the northern positions of some age 5+ CGs are attributable to there being few large values of density in the northwest of the survey area (Figure 3c). In contrast, the CGs of the samples (not presented) weighted by their areas of influence (but not by hake densities) are stable throughout the time-series. Therefore, the differences in location of the CGs between hake age groups could not be attributed to changes in the sampling design and were interpreted as real spatial shifts. Inside each hake age group, scattering of the CGs indicates some interannual variability. Scattering was greatest for the oldest hake group.

The spatial patches were defined using a threshold distance of 100 nautical miles. The mean number of spatial patches for each age group increased slightly, from 1.8 for age 0 hake to 2.46 for age 2, peaked at 2.8 for age 3, then decreased slightly to 2.6 for age 5+ hake (Figure 3a). The main patch of age 0 hake was over the northern continental shelf of the survey area and a lesser one to the south of this but varying in latitude from 1 y to the next (Figure 4). These patches we interpreted as being the nursery areas of the population.

The inertia of the population generally increased with age, indicating a greater spatial dispersion around the CG (Figure 3d).

Isotropy increased from age 0 to age 3, then decreased (Figure 3e). The distribution of hake in the Bay of Biscay seemingly has a preferential direction, more marked at age 0 and age 5+. The direction of age group 0 (Figure 5) was 121°, corresponding roughly to muddy sediment off Brittany (Figure 6). It also corresponded to the line of the CGs (Figure 2). For ages 4 and 5+, the direction was 155° and corresponded to the axis of the slope of the shelf edge, where older hake were mainly concentrated. For the intermediate ages, the population was still anisotropic, probably because of the general shape of the continental shelf, but the state was less marked, indicating maximal isotropy. More or less isotropy may be an indication of how much the spatial distribution of a population component is forced by environmental conditions (bottom sediment, bathymetry, temperature gradient, etc.).

The microstructure index was computed using a mean sample lag of 10 nautical miles. It hardly increased from age 0 to age 2, but

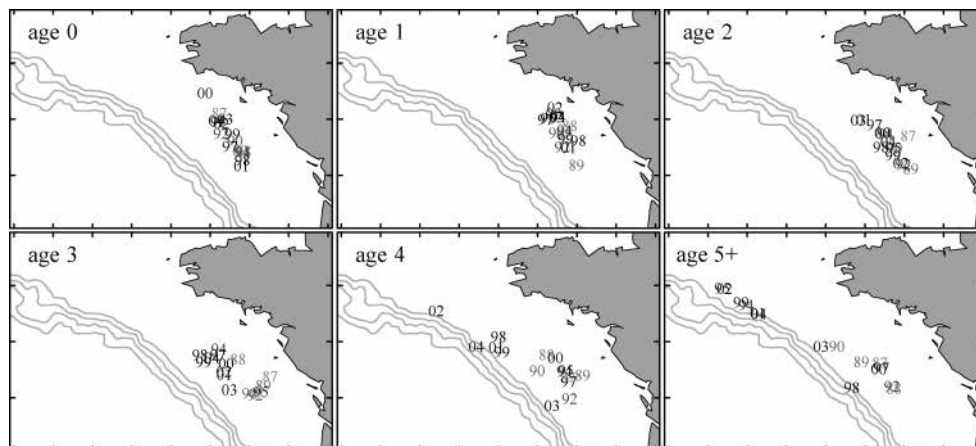


Figure 2. Distribution of the center of gravity of hake age groups computed from 1987 to 2004.

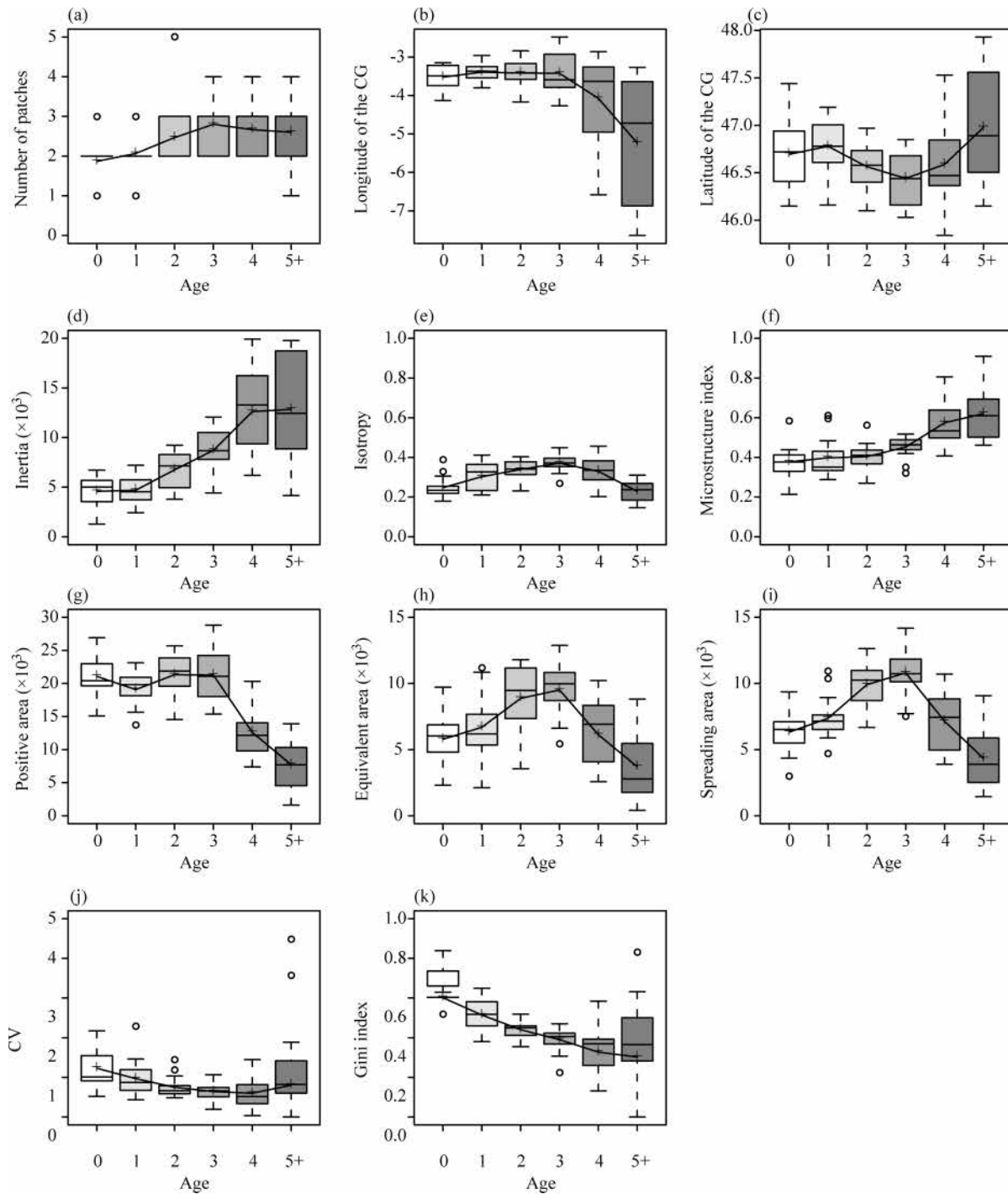


Figure 3. Box plots and means of the spatial indices for age groups 0–5+ . The box stretches from the lower hinge (defined as the 25th percentile or the first quartile Q1) to the upper hinge (defined as the 75th percentile or the third quartile Q3). The median is shown as a line across the box. The mean appears as a cross. The whiskers extend to the farthest points that are not outliers (i.e. that are within 3/2 times the range between quartiles Q1 and Q3). The extreme values defined as outliers are represented by dots. The means are also linked through the ages.

then rose markedly for older ages (Figure 3f). It demonstrated spatial irregularity of fish density increasing with age.

During the study period, the size of the positive area (the area where hake were present) was relatively stable until age 3, then dropped (Figure 3g). Spreading area and equivalent area were closely related (Figure 3h and i). From age 3, they

decreased in a manner similar to that of the positive area. However, in contrast to the positive area, the spreading and equivalent areas increased from age 0 to age 3, showing a better spread of hake aged 3 y.

The CV of strictly positive values decreased from age 0 to age 2 (Figure 3j), whereas the Gini index of strictly positive values

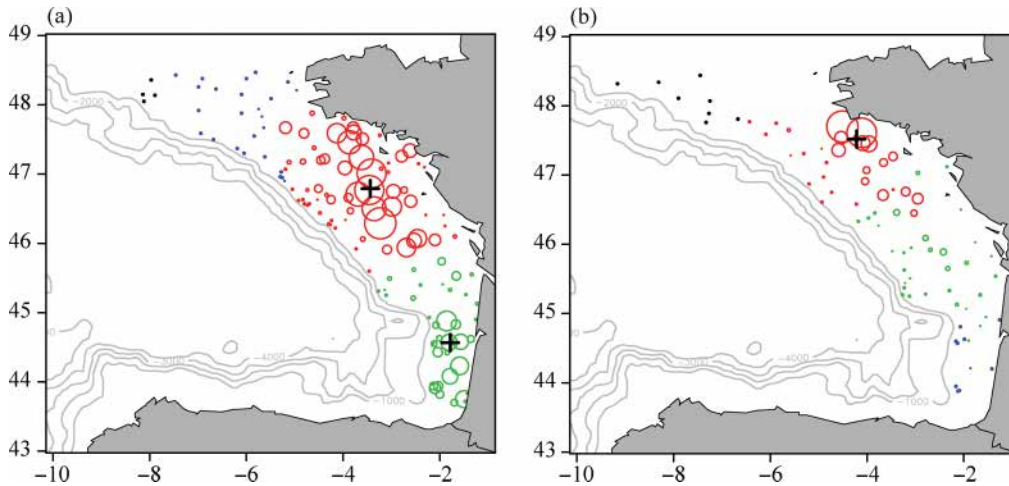


Figure 4. Bubble plot for (a) 1988 and (b) 2000 hake densities, and the corresponding patches (marked by the black cross) defined by a threshold distance of 100 nautical miles and abundance >10% of total abundance. Each sample is shown by a colour indicating the patch to which it belongs.

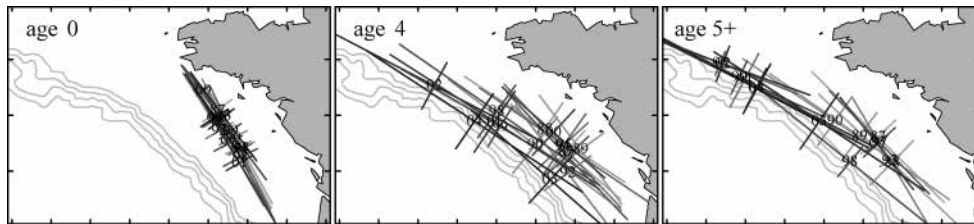


Figure 5. Axes of inertia of hake aged 0, 4, and 5+ computed from 1987 to 2004 showing a distribution with a preferential direction of 121° for age 0 and 155° for ages 4 and 5+. The length of each axis is twice the standard deviation of the projection of population individuals on this axis.

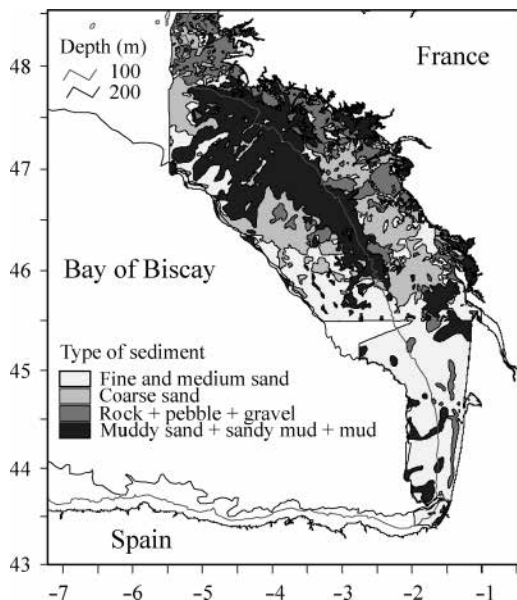


Figure 6. Map of sediments in the Bay of Biscay.

decreased smoothly from age 0 to age 5+, depicting a statistical dispersion that reduced with age (Figure 3k).

The spatial behaviour of hake is strongly linked to its biology. Depth preferences vary throughout a hake’s life (Figure 7), and we recorded an ontogenetic pattern of distribution in which age 0 hake were concentrated almost exclusively between 75 and 125 m, hake aged 1 and 2 in shallower waters over the shelf (25–125 m), and although some older fish were still found on the shelf, a good proportion, increasing with age, was caught at depths of 200–500 m (over the slope). In addition to depth, the nature of the seabed defined yet another ontogenetic pattern of distribution. Young hake (ages 0 and 1) clearly preferred muddy substrata (Figure 8), a preference that was muted with age.

A few more interesting pairwise scatterplots between spatial indices are presented in Figure 9. Inertia and the number of patches varied in the same direction; there were more patches when the spatial dispersion around the CG was larger (Figure 9a). Moreover, older fish dispersed more, mainly to the west of the study area (Figure 9b). The scatterplot of positive area and inertia (Figure 9c) shows that whereas positive area decreased with age, inertia rose with age. Therefore, hake aged 4 and 5+ with extensive spatial dispersion and limited area of presence were in clear contrast to young hake with their broader area of presence and limited spatial dispersion. Both spreading and equivalent areas increased with positive area (Figure 9d and e),

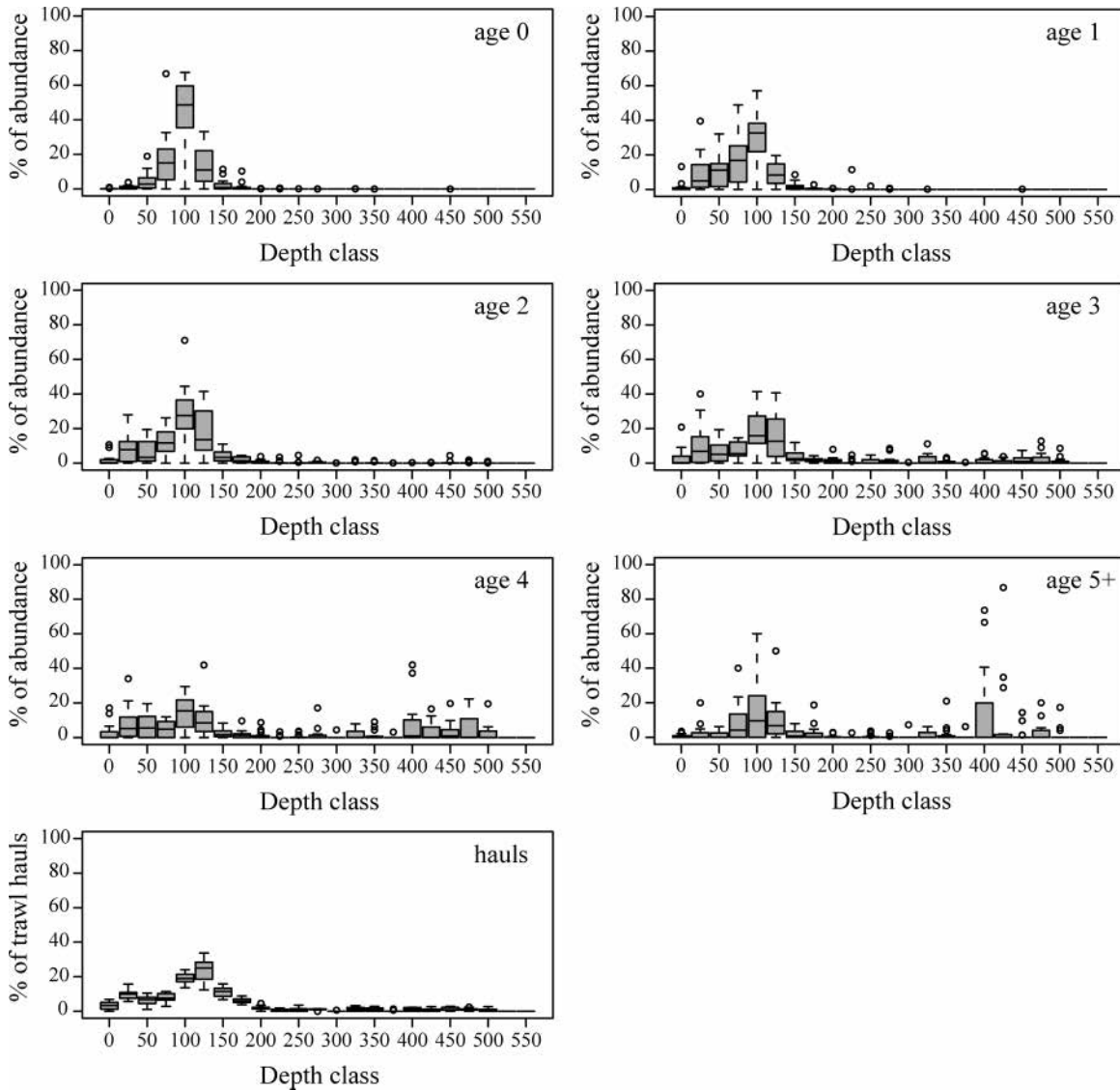


Figure 7. Relative abundance per 25-m depth class for different hake age groups and the proportion of hauls per depth class. The box plot summarizes the distribution for all years per depth class.

in like manner (Figure 9f). However, the microstructure index decreased when the equivalent or spreading areas increased (Figure 9g and h): the fish density surface was more regular when the distribution of hake was more evenly spread.

Comparison of spatial indices: outliers and trends

Our time-series analysis of the indices allowed us to identify the main trends (increase, decrease, stability, no trend) and the years that were different in terms of spatial pattern of hake.

The global index of collocation complements the approach using the CGs and inertia by quantifying the distance between populations. For hake aged 0, for instance, the mean location in 2000 was distant from that of the other years (Table 2). Indeed, the global index of collocation calculated between year 2000 and the others was always lower. It appears that the CG in 2000 was more to the north than in other years (there was no southern patch), testifying to an abnormal distribution that year.

The number of patches of hake aged 0 in each year is of note. One year (1989) had three patches, and 3 y (1987, 2000, and 2002) had just a single patch, instead of the general two patches. Figure 4 shows the patches superimposed on the bubble plots of hake densities for a typical year (1988) and an abnormal year (2000). On average, the main patch was in the northern part of the Bay of Biscay, and the second patch in the southern part, with greater interannual variability according to latitude. In 2000, the second, southern patch was absent. This can be interpreted as poor local recruitment in the area, although the overall level of recruitment in 2000 at the scale of the whole survey area was close to the mean recruitment shown in Table 1. The absence of the second patch in the south in 2000 partly explains the northern position of the CG and the values of the global index of collocation computed between 2000 and other years for hake aged 0.

A decrease in the spreading area through the time-series is detectable for hake aged 4 and 5+ (Figure 10).

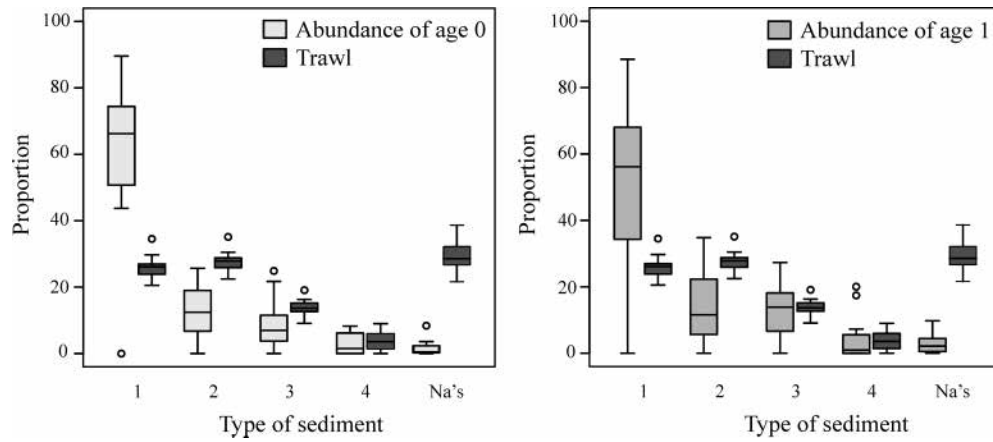


Figure 8. Relative abundance of hake aged 0 and 1 by type of sediment. The number 1 corresponds to mud, sandy mud, and muddy sand, 2 to medium to fine sand, 3 to coarse sand, and 4 to gravel, cobble, and boulder. The notation Na's refers to unknown sediments. The proportion of trawls made in the surveys has been added to the right of the abundance plots for each type of sediment.

Multivariate analysis of hake spatial indices

A multivariate approach is used here to give an overview of the relationship between the different spatial indices and to assess their persistence through time. The components of the hake

population (ages 0 to 5+) being characterized by spatial indices are analysed together.

The first two axes of the MFA accounted for 75% of the total variance in the data. The high value (12.5) of the first eigenvalue

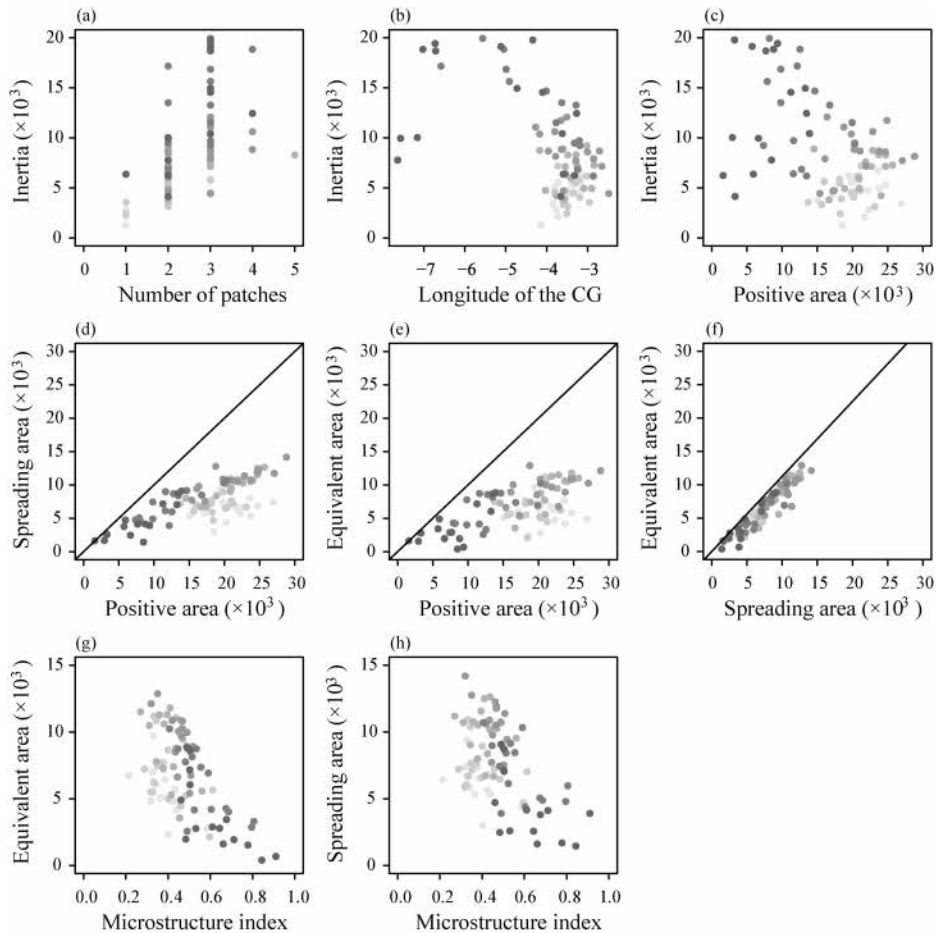


Figure 9. Some pairwise scatterplots between spatial indices (grey varies from light for hake aged 0 to dark grey for hake aged 5+).

Table 2. Global index of collocation computed between any 2 y for hake aged 0.

Year	1987	1988	1989	1990	1992	1994	1995	1997	1998	1999	2000	2001	2002	2003	2004
2004	0.989	0.811	0.846	0.912	0.977	0.829	0.999	0.909	0.79	0.941	0.823	0.769	0.994	0.987	1
2003	0.988	0.844	0.872	0.935	0.973	0.858	0.992	0.919	0.814	0.964	0.8	0.789	0.993	1	
2002	0.975	0.825	0.863	0.932	0.986	0.845	0.998	0.924	0.802	0.961	0.713	0.779	1		
2001	0.719	0.979	0.979	0.939	0.88	0.983	0.805	0.957	0.997	0.898	0.515	1			
2000	0.855	0.521	0.574	0.648	0.761	0.558	0.848	0.654	0.527	0.673	1				
1999	0.913	0.949	0.963	0.994	0.986	0.954	0.96	0.983	0.921	1					
1998	0.742	0.992	0.99	0.958	0.898	0.993	0.826	0.969	1						
1997	0.866	0.979	0.989	0.995	0.977	0.983	0.929	1							
1995	0.989	0.849	0.877	0.934	0.984	0.863	1								
1994	0.786	1	0.999	0.981	0.926	1									
1992	0.947	0.917	0.938	0.976	1										
1990	0.878	0.979	0.987	1											
1989	0.803	0.999	1												
1988	0.764	1													
1987	1														

showed that the first MFA factor represents an important direction of variance for each of the years. The correlation coefficients between the first two MFA factors and the projection of each group of indices (years) were >0.8 (Table 3), indicating that the structuring factors expressed by the first two principal components of MFA were common to all years.

The first two axes of the MFA provide a good representation of the main changes in spatial distribution of hake over its life. The

correlation between the indices and the axes is summarized in Table 4. No index was well enough correlated with axis 3 (see the threshold used in the caption of Table 4) to appear in Table 4. Axis 1 was characterized by the microstructure index, inertia and latitude (positively correlated with axis 1) countering the positive area, spreading area, equivalent area, longitude, Gini index, and the CV of positive densities (negatively correlated with axis 1). Axis 2 was characterized by latitude and the Gini index of positive densities (positively correlated with axis 2) countering the isotropy, spreading area, equivalent area, and the number of patches (negatively correlated with axis 2). Latitude was positively correlated with axes 1 and 2, whereas the spreading and equivalent areas were negatively correlated with both, and the Gini index was

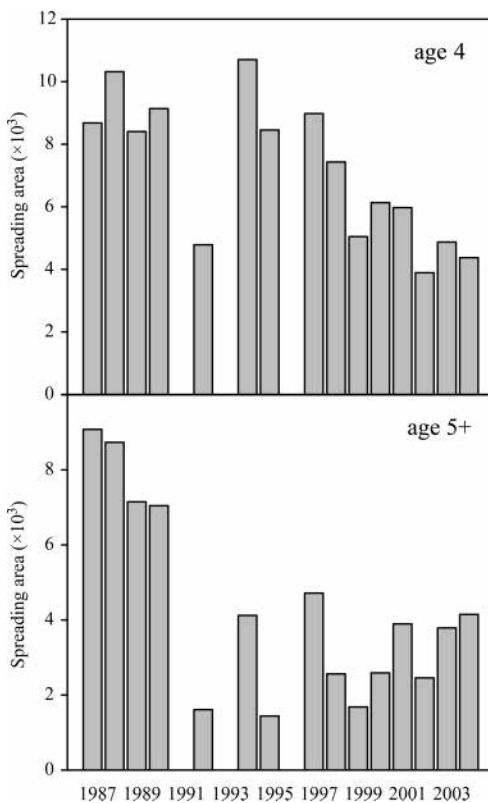


Figure 10. Time-series of spreading area for hake aged 4 and 5+.

Table 3. Multiple factor analysis of 11 spatial indices describing six components (age groups 0–5+) of the hake population of the eastern continental shelf of the Bay of Biscay during 15 survey years.

Year	Axis	
	1	2
1987	0.90	0.84
1988	0.96	0.97
1989	0.99	0.92
1990	0.97	0.96
1992	1.00	0.98
1994	0.82	0.95
1995	0.86	0.80
1997	0.96	0.98
1998	0.99	0.83
1999	0.99	0.95
2000	0.91	0.93
2001	0.98	0.89
2002	0.91	0.86
2003	0.95	0.88
2004	0.98	0.93

Correlation coefficients between the first and second factorial axes are presented as defined from the overall cloud and the projection of the variables of each group (years) defined from the partial clouds.

Table 4. Multiple factor analysis (MFA) of 11 spatial indices describing six components (age groups 0–5+) of the hake population of the eastern continental shelf of the Bay of Biscay during 15 survey years, 1987–2004.

Spatial index	Axis	
	1	2
Longitude of the CG	–(10)	
Latitude of the CG	+(8)	+(8)
Inertia	+(12)	
Isotropy		–(12)
Number of patches		–(8)
Positive area	–(15)	
Spreading area	–(12)	–(10)
Gini index of strictly positive densities	–(11)	+(10)
Equivalent area	–(10)	–(9)
CV of strictly positive densities	–(8)	
Microstructure index	+(13)	

Summary of correlations between variables and the first two MFA factors: –correlation > – 0.4; +correlation < 0.4. The numbers in parenthesis are the number of correlated surveys among the 15 considered in the study. Indices are listed only when the number of correlated surveys is > 8 per index.

positively correlated with axis 2 and negatively with axis 1. The other indices more specifically correlated with just one axis.

The main spatial features of hake age groups are summarized in Figure 11. Two groups can be identified from their scores on axis 1: the younger ages, 0–3, and the older ages, 4 and 5+. With respect to axis 1, older ages were farther west than younger ones, with a higher microstructure index and inertia, but a smaller positive area and CV of positive densities. Age 3 yielded the largest spreading and equivalent areas (axes 1 and 2), as well as peak isotropy and most patches (axis 2). Finally, the location of age 0 hake corresponded

to a higher Gini index of positive densities, whereas the location of age 5+ corresponded to a more northerly distribution. The year-on-year variability by age (the size of the “stars” in Figure 11) decreased from age 0 to 3, but increased again for ages 4 and 5+.

The position of the years in the MFA principal plane (Figure 12) is explained by the correlation between the axes and the variables (Table 3). Three groups of years could be identified: two had high scores on axis 1 (>0.75), and the third (1994, 2000, 1995, 1987, and 2002) had low scores on axis 1 and highly variable ones on axis 2. The first two groups could be distinguished on axis 2: a group including surveys carried out mainly at the beginning of the series (1988–1990, 1992, and 1997), and another group of later surveys (1998, 1999, 2001, 2003, and 2004). The latter group was characterized by smaller statistical dispersion, more patches, higher isotropy, a greater spreading area and equivalent area, and a more southerly distribution.

The year 1994 most often stood apart from the CGs of the age groups (Figure 11). The MFA factor 2 was in that case a more critical structuring direction (Table 3, and age groups 5+ and 2 in Figure 11) than factor 1 (age groups 4 and 1 in Figure 11). The explanation would be similar for 2000 and, to a lesser extent, 1995. Notable age groups were 0 for 2000 and 0, 4, and 5+ for 1995 (Figure 11).

Discussion

A set of spatial indices is proposed to describe in a simple fashion the spatial patterns of a fish population from survey data. Such a set should not be considered fixed, the idea being rather to combine several basic statistics to describe different features of the spatial population. Some indices actually depend on the location where a particular value of density was observed: these were the CG and associated statistics (inertia and isotropy), the

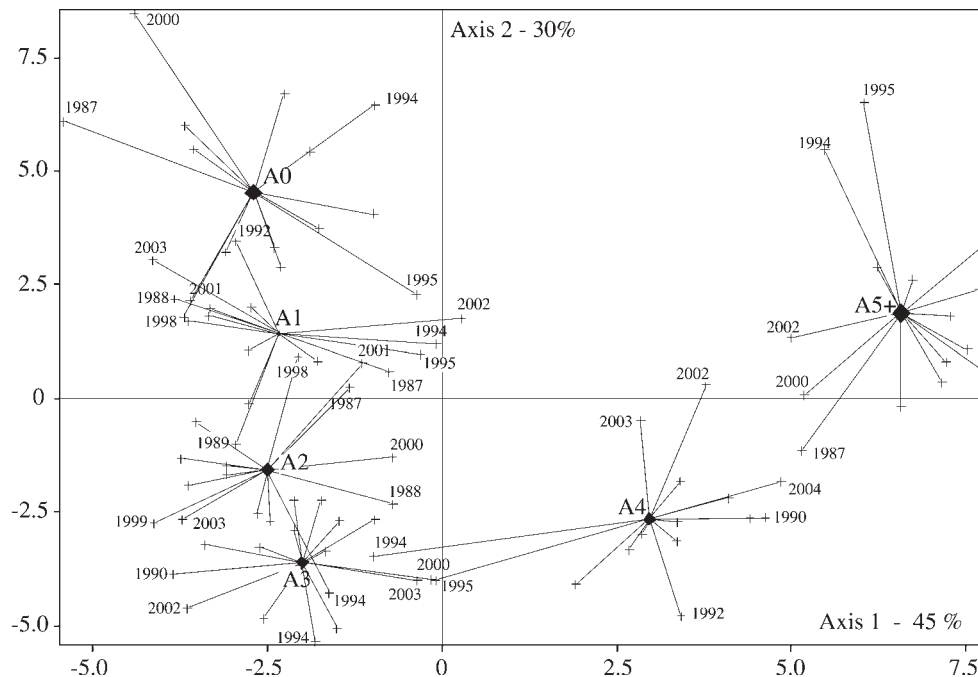


Figure 11. Graphical depiction of the projections of hake age groups on the principal multiple factor analysis plane. Diamonds represent the CG of age groups observed during 15 surveys. Symbol size is proportional to an age group’s contribution to the construction of the axes. Plus signs indicate the position of each age group in the relevant year.

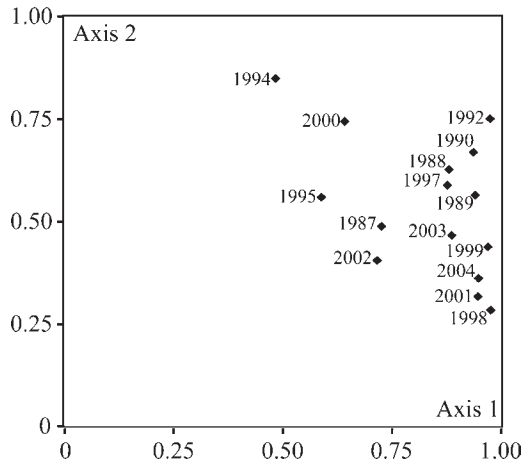


Figure 12. Multiple factor analysis (MFA) of 11 spatial indices describing six components (age groups 0–5+) of the hake population of the eastern continental shelf of the Bay of Biscay. Projections of the years sampled on the principal MFA plane show the relationships between them from an overall point of view.

spatial patches, the microstructure index, and the statistics of parameters for the population (e.g. mean depth). Other statistics only describe statistical distributions and would not be changed by permutation of the values of a variable between sample locations (providing that associated areas of influence are the same). They include all area indices and the statistics describing the histogram of fish density values (e.g. the CV of strictly positive values). However, the histogram of fish density values includes a spatial aspect through the underlying support on which density is measured (e.g. the area swept by the trawl). Note that the microstructure index, the CV of positive values, and the positive area, for instance, depend on the size of this support.

Because of the potential problem posed by zero values of density (i.e. which values should be included in the domain), the indices were selected so as not to be affected by zero values. This is true for all statistics weighted by density, each individual of a population being given the same weight (this includes the CG and its associated statistics). Such a weighting has another advantage, namely the lack of sensitivity of the statistics to a low value of density. For instance, one low-density value makes a small contribution to the CG, but several low-density values may make a significant contribution. In contrast, each low density value makes a greater contribution to the CV and the Gini index of strictly positive density values and a full contribution to the positive area.

The CGs of surveys (CG of samples, weighted by the areas of influence, but not by fish densities) showed very little change. Therefore, the differences in the location of the CGs between and within hake age groups may be interpreted as spatial shifts between and within the hake population components.

An important point, not addressed statistically herein, is the precision of the proposed indices when they are estimated from survey data. For example, what is the precision of the CG estimated from the fish density values of a survey? Resampling procedures can yield the sensitivity of the CG to data values. However, a hypothesis of spatial continuity is required to relate the values of fish density at sample points to unknown values over the space that defines the true CG. Geostatistical simulations may offer a

solution, the price being in the very strong hypotheses required to do so. Here, the precision of spatial indices is somewhat bypassed by considering repetition in time through the evolution of the time-series, in which a sustainable trend or a change of level is likely to be significant. However, the precision would be the important issue if, for instance, the CG of the population next year lay away from where it was formerly, and if this was not attributable to a problem in spatial sampling.

Spatial indices selected or developed here allow us to capture the spatial patterns of hake. Young hake aggregate and are spatially well structured. There are generally two patches of hake aged 0, on the muddy substrata of the eastern central continental shelf of the Bay of Biscay. The spatial pattern of hake aged 0 is related to reproduction of the species over the slope, and to the transport of eggs and larvae towards a habitat suitable for their development. Alvarez *et al.* (2004) suggest that the transport of the hake larvae to nursery areas is controlled by hydrographic mechanisms such as geostrophic currents in the Bay of Biscay and tidal currents in the north. The variability of such mechanisms may influence the survival of the larvae and hence the recruitment strength, which in turn affects the spatial pattern of age group 0.

Crustaceans (mainly euphausiids) are the main components of young hake diet (Guichet, 1995; Velasco and Olaso, 1998) in the Bay of Biscay and the Cantabrian Sea. The proportion of crustaceans and fish in the diet changes markedly when hake attain ~20 cm and 1 y of age (Kacher, 2004). Then, hake become almost exclusively piscivorous and leave the nursery grounds. However, the global index of collocation between age groups 0 and 1 (between 0.839 and 0.998 through the study period) show that their spatial distributions overlap significantly. Therefore, hake aged 1 are no longer associated with nursery grounds, although their spatial distribution remains almost unchanged.

Subsequently, the spatial pattern of hake changes, and fish aged 3 y are more homogeneously distributed over the whole shelf. The number of patches, the isotropy, and the equivalent and spreading areas peak. Inertia and the microstructure index increase with age, whereas the CV and the Gini index decrease. Age 3 appears to be a turning point at which hake change the way in which they occupy space. The oldest hake groups in our study (age 4 and 5+) move offshore towards the western Bay of Biscay (note the CG) and are caught mainly along the edge of the continental shelf (where their densities are greatest). Their spatial distribution is less structured (a low microstructure index), less isotropic (low isotropy), and individual fish are more scattered while they occupy a reduced area (high inertia, large number of patches, and a small positive area). As well as the positive area, the equivalent and spreading areas decrease between age groups 3 and 5+. The spatial distribution of hake is marked by a preferential direction, more marked for youngest and oldest age groups (less isotropy). For age group 0, the shape of the muddy substrata defines the direction, because hake seemingly prefer such a substratum (proportion of abundance per type of sediment). For hake aged 5+, the continental shelf edge provides the direction, although hake inhabit deeper water as they get bigger and older (relative abundance per depth class).

Several of these results were already known. The nursery areas for European hake were already documented as being in coastal, relatively shallow water over muddy substrata in the northern Bay of Biscay, known as “la Grande Vasière” (Dardignac, 1988; Bez *et al.*, 1995). Another known nursery area is in the south-eastern corner of the Bay of Biscay (2°W) (Sanchez, 1994). The

spatio-temporal dynamics of hake aged 0 are described by Petitgas (1998), and information on the distribution of adult hake is given by Poulard (2001). This work gives information on the spatial distribution of intermediate age groups and provides an overview of space occupation by different age groups of hake. A multivariate approach permits us to produce results combining all age groups and years (Figure 11), and to identify trends and outliers that exist in the time-series (Figure 12). Therefore, the ontogenetic pattern of hake seen here seems to be a prevailing characteristic for the stock. Age group 3 appears to mark a key point in the spatial dynamics of the hake population and could be linked to the maturation cycle. Males attain maturity smaller and younger than females (~39 cm and 3.4 y, and ~47 cm and 4.2 y, respectively; ICES, 2005). Regarding depth preference, the ontogenetic pattern of distribution that we observed has also been found for Mediterranean hake, age 0 fish being distributed almost exclusively at depths of 100–250 m, intermediate ages (mainly 1-y-olds) being concentrated shallower, and older hake generally being found over the continental slope (Abella *et al.*, 2005).

Data were sourced from standardized surveys, the same gear being used throughout and survey conditions not varying significantly. The Bay of Biscay is generally sampled within a period of 1 month, so year-on-year data are generally comparable in terms of a uni-seasonal signal. However, the set of data provided by autumn surveys does not permit description of seasonal changes in spatial distribution. Therefore, our approach is limited to identifying and quantifying such interannual variations in the spatial pattern observed during autumn surveys only. We need to bear in mind the fact that spatial indices depend on standardized monitoring and can be upset by changes to gear (selectivity and catchability linked to age). However, the patterns may at least partly reflect reality (e.g. the shift of the CGs with age, increased dispersion by age). Of course, this statement applies to any use of survey data.

Finally, spatial indices allow us to capture and to detect changes over time in the spatial pattern of a fish population. They improve our understanding of the spatial dynamics of a population in a quantitative manner. A follow-up step would be to investigate the spatial behaviour of a population in relation to changes in abundance. Potential relationships between spatial indices and fish population dynamics might be expected, and these may be of value in developing new assessment tools and management procedures, in which the spatial patterns of a stock are considered. This could help move towards assessment advice and quota allocation given on a spatially disaggregated basis and allow management authorities to consider the closure of specific areas to fishing when deemed necessary. Spatial management with appropriate tools is required (Babcock *et al.*, 2005) where resources are highly impacted by fishing.

Acknowledgements

The study was carried out with the financial support of the European Union (project FISBOAT—Fisheries Independent Survey Based Operational Assessment Tools, DG—Fish, 6th Framework STREP, Contract 502572).

References

Abella, A., Serena, F., and Ria, M. 2005. Distributional response to variations in abundance over spatial and temporal scales for juveniles of European hake (*Merluccius merluccius*) in the western Mediterranean Sea. *Fisheries Research*, 71: 295–310.

- Alvarez, P., Fives, J., Motos, L., and Santos, M. 2004. Distribution and abundance of European hake *Merluccius merluccius* (L.), eggs and larvae in the Northeast Atlantic waters in 1995 and 1998 in relation to hydrographic conditions. *Journal of Plankton Research*, 26: 811–826.
- Atkinson, D. B., Rose, G. A., Murphy, E. F., and Bishop, C. A. 1997. Distribution and abundance of northern cod, 1981–1993. *Canadian Journal of Fish and Aquatic Sciences*, 54: 132–138.
- Babcock, E. A., Pikitch, E. K., McAllister, M. K., Apostolaki, P., and Santora, C. 2005. A perspective on the use of spatialized indicators for ecosystem-based fishery management through spatial zoning. *ICES Journal of Marine Science*, 62: 469–476.
- Bez, N. 1997. Statistiques individuelles et géostatistique transitive en écologie halieutique. Thèse de Docteur en Géostatistique, Ecole Nationale Supérieure des Mines de Paris, France. 276 pp.
- Bez, N., and Rivoirard, J. 2000. Indices of collocation between populations. *In* Report of a Workshop on the Use of Continuous Underway Fish Egg Sampler (CUFES) for Mapping Spawning Habitat of Pelagic Fish, pp. 48–52. Ed. by D. M. Checkley, J. R. Hunter, L. Motos, and C. D. von der Lingen. GLOBEC Report, 14.
- Bez, N., and Rivoirard, J. 2001. Transitive geostatistics to characterize spatial aggregation with diffuse limits: an application on mackerel ichthyoplankton. *Fisheries Research*, 50: 41–58.
- Bez, N., Rivoirard, J., Guiblin, Ph., and Walsh, M. 1997. Covariogram and related tools for structural analysis of fish survey data. *In* Geostatistics Wollongong '96, 2, pp. 1316–1327. Ed. by E. Y. Baafi, and N. A. Schofield. Kluwer, Dordrecht.
- Bez, N., Rivoirard, J., and Poulard, J.-C. 1995. Approche transitive et densité de poissons. *Compte-rendu des journées de Géostatistiques*, 15–16 juin 1995, Fontainebleau, France. *Cahier de Géostatistique*, 5: 161–177.
- Brodie, W. B., Walsh, S. J., and Atkinson, D. B. 1998. The effect of stock abundance on range contraction of yellowtail flounder (*Pleuronectes ferruginea*) on the Grand Bank of Newfoundland in the Northwest Atlantic from 1975 to 1995. *Journal of Sea Research*, 39: 139–152.
- Crecco, V., and Overholtz, W. J. 1990. Causes of density-dependent catchability of Georges Bank haddock *Melanogrammus aeglefinus*. *Canadian Journal of Fisheries and Aquatic Sciences*, 47: 385–394.
- Dardignac, J. 1988. Les pêcheries du Golfe de Gascogne—Bilan des connaissances. *Rapports scientifiques et techniques de l'IFREMER*, 9. IFREMER Editions, Paris.
- DECISIA. 2003. SPAD, système pour l'analyse des données, version 5.6.0. CISIA-CERESTA, Montreuil.
- Drouineau, H., Mahévas, S., Pelletier, D., and Beliaeff, B. 2006. Assessing the impact of different management options using ISIS—Fish: the French *Merluccius merluccius*–*Nephrops norvegicus* mixed fishery of the Bay of Biscay. *Aquatic Living Resources*, 19: 15–29.
- Escofier, B., and Pagès, J. 1994. Multiple factor analysis (AFMULT package). *Computational Statistics and Data Analysis*, 18: 121–140.
- Garrison, L. P., and Link, J. S. 2000. Fishing effects on spatial distribution and trophic guild structure of the fish community in the Georges Bank region. *ICES Journal of Marine Science*, 57: 723–730.
- Gini, C. 1921. Measurement of inequality and incomes. *The Economic Journal*, 31: 124–126.
- Greenstreet, S. P. R., and Hall, S. J. 1996. Fishing and the ground-fish assemblage structure in the north-western North Sea: an analysis of long-term and spatial trends. *Journal of Animal Ecology*, 65: 577–598.
- Guichet, R. 1995. The diet of European hake (*Merluccius merluccius*) in the northern part of the Bay of Biscay. *ICES Journal of Marine Science*, 52: 21–31.

- Hollowed, A. B. 1992. Spatial and temporal distribution of Pacific hake, *Merluccius productus*, larvae and estimates of survival during early life stages. CalCOFI Report, 33: 100–123.
- ICES. 1997. Report of the International Bottom Trawl Survey Working Group (IBTSWG). ICES Document CM 1997/H: 6. 50 pp.
- ICES. 2005. Report of the Working Group on the Assessment of Hake, Monk and Megrim (WGHMM), 10–19 May 2005, Lisbon, Portugal. ICES Document CM 2006/ACFM:01. 67 pp.
- Kacher, M. 2004. Le merlu du golfe de Gascogne et de la mer Celtique: croissance, répartition spatiale et bathymétrique, écologie alimentaire et assemblages. Thèse de 3ème cycle, Université du Littoral Côte d'Opale. 192 pp.
- Kendall, A. W., and Picquelle, S. J. 1989. Egg and larva distributions of walleye pollock *Theragra chalcogramma* in Shelikof Strait, Gulf of Alaska. Fishery Bulletin US, 88: 133–154.
- MacCall, A. D. 1990. Dynamic Geography of Marine Fish Populations. University of Washington Press, Seattle. 153 pp.
- Marshall, C. T., and Frank, K. T. 1994. Geographic responses of groundfish to variation in abundance: methods of detection and their implication. Canadian Journal of Fish and Aquatic Sciences, 51: 808–816.
- Matheron, G. 1971. The theory of regionalized variables and its applications. Les cahiers du Centre de Morphologie Mathématique, Fascicule 5. Ecole Nationale Supérieure des Mines de Paris, Paris. 212 pp.
- Matheron, G. 1981. La sélectivité des distributions. Rapport du CGMM, Ecole Nationale Supérieure des Mines de Paris, Paris. 45 pp.
- Matheron, G. 1985. Comparaison de quelques distributions du point de vue de la sélectivité. Rapport du CGMM, Ecole Nationale Supérieure des Mines de Paris, Paris. 20 pp.
- McFarlane, G. A., King, J. R., and Beamish, R. J. 2000. Have there been recent changes in climate? Ask the fish. Progress in Oceanography, 47: 147–169.
- Murawski, S. A., and Finn, J. T. 1988. Biological bases for mixed species fisheries: species co-distribution in relation to environmental and biotic variables. Canadian Journal of Fish and Aquatic Sciences, 45: 1720–1735.
- Myers, R. A., and Cadigan, N. G. 1995. Was an increase in natural mortality responsible for the collapse of northern cod? Canadian Journal of Fish and Aquatic Sciences, 52: 1274–1285.
- Pagès, J., and Husson, F. 2001. Inter-laboratory comparison of sensory profiles: methodology and results. Food Quality and Preference, 12: 297–309.
- Petitgas, P. 1998. Biomass-dependent dynamics of fish spatial distributions characterized by geostatistical aggregation curves. ICES Journal of Marine Science, 55: 443–453.
- Poulard, J.-C. 2001. Distribution of hake (*Merluccius merluccius*, Linnaeus, 1758) in the Bay of Biscay and the Celtic Sea from the analysis of French commercial data. Fisheries Research, 50: 173–187.
- Poulard, J.-C., and Blanchard, F. 2005. The impact of climate change on the fish community structure of the eastern continental shelf of the Bay of Biscay. ICES Journal of Marine Science, 62: 1436–1443.
- Poulard, J.-C., Blanchard, F., Boucher, J., and Souissi, S. 2003. Variability in the demersal fish assemblages of the Bay of Biscay during the 1990s. ICES Marine Science Symposia, 219: 411–414.
- Roessig, J. M., Woodley, C. M., Cech, J. J., and Hansen, L. J. 2004. Effects of global climate change on marine and estuarine fishes and fisheries. Reviews in Fish Biology and Fisheries, 14: 251–275.
- Sanchez, F. 1994. Patronos de distribución y abundancia de la merluza en aguas de la plataforma norte de la Península Iberica. In Jornadas Sobre el Estado Actual de los Conocimientos de las Poblaciones de Merluza que Habitan la Plataforma Continental Atlantica y Mediterranea de la Union Europea con Especial Atencion a la Península Iberica, pp. 255–279. Ed. by A. Gonzalez-Garces, and F. J. Pereira. Publicacion Privada.
- Stanimirova, I., Walczak, B., and Massart, D. L. 2005. Multiple factor analysis in environmental chemistry. Analytica Chimica Acta, 545: 1–12.
- Swain, D. P., and Wade, E. J. 1993. Density-dependent geographic distribution of Atlantic cod in the southern Gulf of St Lawrence. Canadian Journal of Fisheries and Aquatic Sciences, 50: 725–733.
- Swain, D. P., and Sinclair, A. F. 1994. Fish distribution and catchability: what is the appropriate measure of distribution? Canadian Journal of Fisheries and Aquatic Sciences, 51: 1046–1054.
- Swain, D. P., and Morin, R. 1996. Relationships between geographic distribution and abundance of American plaice (*Hippoglossoides platessoides*) in the southern Gulf of St Lawrence. Canadian Journal of Fisheries and Aquatic Sciences, 53: 106–119.
- Velasco, F., and Olaso, I. 1998. European hake *Merluccius merluccius* (L., 1758) feeding in the Cantabrian Sea: seasonal, bathymetric and length variations. Fisheries Research, 38: 33–44.

Appendix

Matheron (1985) studied the relationship between the index of selectivity (or Gini index, denoted G herein) and the coefficient of variation $CV = \sigma/m$ of a probability distribution function F . For a non-negative distribution F , he obtained the following inequalities (p. 19):

$$G \leq \frac{CV}{\sqrt{3}}, \quad (18)$$

with equality iff F is uniform (then $CV^2 \leq 1/3$), and

$$G \leq 1 - \frac{8}{9(1 + CV^2)}, \quad (19)$$

with equality iff F is uniform on an interval $(0, L)$ with an atom at the origin (then $CV^2 > 1/3$).

These relations can be transposed to the strictly positive values of the distribution of a population density using Equations (10) and (16). Relation (18) gives

$$\frac{EA}{PA} \leq \frac{1}{1 + 3(1 - SA/PA)^2} \quad (20)$$

with equality iff F is uniform (then $3/4 \leq EA/PA \leq 1$, and $2/3 \leq SA/PA \leq 1$). Relation (19) gives

$$\frac{EA}{PA} \leq \frac{9SA}{8PA}, \quad (21)$$

with equality iff F is uniform on an interval $(0, L)$ (then $EA/PA = 3/4$, and $SA/PA = 2/3$). Inequality (21) is stronger than (20) if $SA/PA \leq 2/3$, i.e. $EA/PA \leq 3/4$, and (20) stronger than (21) if $2/3 \leq SA/PA$, i.e. $3/4 \leq EA/PA \leq 1$. However, the most remarkable result is the simple inequality between the equivalent area and the spreading area obtained from (21):

$$EA \leq \frac{9}{8}SA, \quad (22)$$

with equality iff F is uniform on the interval $(0, L)$.